Calcium Signaling of *in situ* Chondrocytes in Articular Cartilage under Compressive Loading: Roles of Calcium Sources and Cell Membrane Ion Channels

Mengxi Lv[1], **Yilu Zhou**[1], **Xingyu Chen**[1], **Lin Han**[2], **Liyun Wang**[1], and **X Lucas Lu**[1,*]

[1]Department of Mechanical Engineering, University of Delaware, Newark, DE 19716

[2]School of Biomedical Engineering, Science, and Health Systems, Drexel University, Philadelphia, PA 19104

Abstract

Mechanical loading on articular cartilage can induce many physical and chemical stimuli on chondrocytes residing in the extracellular matrix (ECM). Intracellular calcium ($[Ca^{2+}]_i$) signaling is among the earliest responses of chondrocytes to physical stimuli, but the $[Ca^{2+}]_i$ signaling of *in situ* chondrocytes in loaded cartilage is not fully understood due to the technical challenges in $[Ca^{2+}]_i$ imaging of chondrocytes in a deforming ECM. This study developed a novel bi-directional microscopy loading device that enables the record of transient $[Ca^{2+}]_i$ responses of *in situ* chondrocytes in loaded cartilage. It was found that compressive loading significantly promoted $[Ca^{2+}]_i$ signaling in chondrocytes with faster $[Ca^{2+}]_i$ oscillations in comparison to the non-loaded cartilage. Seven $[Ca^{2+}]_i$ signaling pathways were further investigated by treating the cartilage with antagonists prior to and/or during the loading. Removal of extracellular Ca^{2+} ions completely abolished the $[Ca^{2+}]_i$ responses of *in situ* chondrocytes, suggesting the indispensable role of extracellular Ca^{2+} sources in initiating the $[Ca^{2+}]_i$ signaling in chondrocytes. Depletion of intracellular Ca^{2+} stores, inhibition of PLC-IP$_3$ pathway, and block of purinergic receptors on plasma membrane led to significant reduction in the responsive rate of cells. Three types of ion channels that are regulated by different physical signals, TRPV4 (osmotic and mechanical stress), T-type VGCCs (electrical potential), and mechanical sensitive ion channels (mechanical loading) all demonstrated critical roles in controlling the $[Ca^{2+}]_i$ responses of *in situ* chondrocyte in the loaded cartilage. This study provided new knowledge about the $[Ca^{2+}]_i$ signaling and mechanobiology of chondrocytes in its natural residing environment.

Keywords

Cartilage Explant; Mechanotransduction; Calcium Source; T-type VGCC; TRPV4

*Corresponding Author: X. Lucas Lu, Ph.D. Department of Mechanical Engineering, University of Delaware, 130 Academy Street, Newark, DE 19716, Telephone: (302) 831-3581, xlu@udel.edu.

Disclosure: All authors have no conflicts of interest.

Conflict of Interest Statement

All authors state that they have no conflicts of interest.

1. INTRODUCTION

Chondrocytes are the sole cell type in articular cartilage and responsible for the biosynthesis and catabolism of extracellular matrix (ECM). Metabolic activities of chondrocytes can be regulated by the physical stimuli induced by the daily mechanical loading on cartilage (1). Due to the multi-phasic nature of cartilage, compressive loading on cartilage can generate changes in mechanical, hydrostatic, chemical, and electrical signals across the tissue (2; 3). Oscillation of intracellular calcium ($[Ca^{2+}]_i$) concentration is among the earliest and most fundamental molecular responses of chondrocytes to most physical stimuli, including compression (4–6), fluid flow (7), hydrostatic pressure (8), osmotic stress (9–11) and electric current (12), as shown by previous studies using monolayer chondrocytes or chondrocytes seeded in hydrogels. Calcium signaling plays significant roles in numerous biological functions including cell adhesion, metabolism, secretion, proliferation and apoptosis (13). Recent studies found that chondrocytes have spontaneous $[Ca^{2+}]_i$ signaling without the presence of any exotic stimuli (11; 14; 15), suggesting the fundamental roles of $[Ca^{2+}]_i$ in modulating the biological processes and metabolic activities within chondrocytes.

At rest status, cells maintain a 20,000-fold gradient of Ca^{2+} concentration between the intracellular (~100 nM) and extracellular space (~mM) (16). The rapid $[Ca^{2+}]_i$ ascent in cytosol mainly relies on two mechanisms, Ca^{2+} influx from the extracellular environment and the release from intracellular Ca^{2+} stores such as endoplasmic reticulum (ER). In chondrocytes, both mechanisms play essential roles in regulating the physical stimuli-induced $[Ca^{2+}]_i$ responses (4). Several types of channels on chondrocytes membrane, such as transient receptor potential vanilloid channels (e.g., TRPV4 channel) (10), mechanosensitive ion channels (e.g., PIEZO channels) (17), and voltage gated calcium channels (e.g., T-type VGCC) (18), can be activated by various physical stimuli and lead to extracellular Ca^{2+} influx in milliseconds. Physical stimuli and Ca^{2+} influx can also trigger the release of adenosine triphosphate (ATP) from membrane vesicles into the extracellular space and activate the purinergic receptors (*e.g.*, P2Y family) and ligand gated ion channels (*e.g.*, P2X family) on plasma membrane (19). Activation of P2Y receptors can subsequently stimulate the activation of intracellular phospholipase C (PLC) and the generation of inositol 1,4,5-trisphosphate (IP$_3$), which can bind to the IP$_3$ receptors on ER and induce rapid Ca^{2+} release into cytosol. The PLC-IP$_3$ pathway can also be activated by many other G protein-couple receptors or even mechanical stress on the cell membrane (20).

Most studies on chondrocyte $[Ca^{2+}]_i$ signaling were performed on short-term monolayer cultured cells, freshly-isolated cells, and cells seeded in hydrogel constructs (4; 21–24). The unnatural residing environment can significantly affect chondrocyte phenotype, metabolic activities, and mechanotransduction behaviors (25). However, imaging of *in situ* chondrocytes in their native ECM, when cartilage is under mechanical loading, remains technically challenging. Loading on cartilage often incurs large, long lasting, and inconstant speed displacement of cells exceeding the imaging field of microscope. In light of a novel microscopy indentation system, Madden et al. first investigated the calcium signaling of *in situ* chondrocytes residing in the superficial zone using intact cartilage-bone explants. The calcium signaling of *in situ* chondrocytes during and immediately after indenting showed a unique correlation pattern with the loading magnitude and also differed in cartilage from

femoral condyle and patellar regions (5). These findings proved that the calcium signaling of chondrocytes can significantly depend on their surrounding environment and the loading profiles, which intrigued further questions such as how *in situ* chondrocytes respond during the loading phase and how the calcium responses depend on the aforementioned essential calcium sources and ion channels. As the phenotype of chondrocytes changes along depth, mature chondrocytes may also have different mechanotransduction characters with the pre-mature chondrocytes in the superficial zone. In this study, a custom-designed microscopy loading device was built to apply controlled mechanical loading on cartilage explant, so that the $[Ca^{2+}]_i$ transient of *in situ* mature chondrocytes can be recorded during the loading phase. $[Ca^{2+}]_i$ responses were compared with the spontaneous $[Ca^{2+}]_i$ signaling of chondrocytes in terms of spatiotemporal characteristics. Moreover, roles of seven essential pathways related to $[Ca^{2+}]_i$ signaling were investigated in the loading induced $[Ca^{2+}]_i$ responses of *in situ* chondrocytes.

2. MATERIALS AND METHODS

2.1. Cartilage Explant

Cartilage samples were harvested from the central region of femoral condyle heads of fresh calf knee joints (3-6 months old) with mixed gender and side (six joints from Green Village, NJ). The full thickness of cartilage was approximately 5–6 mm. Cylindrical explants (diameter = 3 mm, thickness = 2 mm) from the middle zone cartilage were isolated using a biopsy punch and a custom-designed cutting tool (15). After harvest, samples were balanced and cultured in DMEM supplemented with 1% ITS+Premix, 50 μg/ml L-proline, 0.1 μM dexamethasone, 0.9 mM sodium pyruvate and 50 μg/ml ascorbate 2-phosphate at 37 °C and 100% humidity for 3 days before use (11; 15). Dexamethasone was added in the culture medium to preserve the mechanical integrity of calf cartilage explant (26). On the day of calcium imaging, each cartilage explant was halved axially by a cutting tool (ASI-Instruments, MI) and stained in the fluorescent calcium dye solution, DMEM with 5 μM Fluo-8 AM (AAT Bioquest, CA) at 37°C for 40 minutes. Afterwards samples were gently washed in pure DMEM three times with 10 minutes each time. The half-cylindrical cartilage sample, with the cross-section area facing down, was then placed in a glass-slide imaging chamber, which itself was secured on a microscopy-loading device as described below.

2.2. Mechanical Loading and Calcium Imaging

A unique loading device was designed and built to apply mechanical loading on cartilage samples during the microscopy imaging (Fig. 1A–B). Each of the two opposing loading platens, locating in the imaging chamber, was driven by a high-resolution (0.016 μm) linear actuator (M-235.5DG, Physik Instrumente, Germany). The two identical actuators, aligned along the same axis, are controlled by two independent servo controllers (C863, Physik Instrumente, Germany). Cartilage samples placed between the two loading platens were compressed from both sides at identical speed (Fig. 1C). Displacement of the central region in the explant was offset by the opposing movement of two actuators, which allowed a relatively steady imaging area during the time course of imaging. A miniature load cell (Model 31, Sensotec Inc., Columbus, OH, USA; range 0–10 lbs) was mounted between a loading platen and the corresponding actuator to record the transient resisting forces from

the cartilage (Fig. 1D). The entire loading device can be secured on the XY stage of a confocal microscope (Zeiss LSM510) to record the fluorescent images of *in situ* chondrocytes.

During the test, a 0.5 N (0.14 MPa) tare load was first applied to the sample to ensure the full contact between loading platens and cartilage, followed by a 10-minute resting period for cells to recover from previous agitation (27; 28). The center region of the explant was imaged at a focal plane ~30 μm deeper below the cross-section surface, which avoided the cells damaged by previous cutting. During calcium imaging, each loading platen was driven at the speed of 0.1 μm/s for 1000 seconds to reach ~10% final strain, and the real time fluorescent images of the chondrocytes were captured every 1.5 s by confocal microscope during the loading. To compare the mechanically induced $[Ca^{2+}]_i$ responses to the spontaneous $[Ca^{2+}]_i$ signaling in chondrocytes, a half explant was imaged following protocols described above, while the other half was imaged without loading and served as the non-loaded control.

2.3. Calcium Signaling Pathways

To understand the molecular mechanisms of the loading-induced $[Ca^{2+}]_i$ responses in chondrocytes, extra cartilage samples were harvested and separated into seven groups. Each sample was cut into two halves and stained in calcium dye solution. A half explant was treated with a specific pathway antagonist 30 min prior to and/or during the calcium imaging, while the other half was incubated in DMEM and served as the untreated control. (1) Extracellular Ca^{2+} source: After Fluo-8 AM dye, cartilage sample was transferred into calcium-free DMEM for imaging. EGTA, a Ca^{2+} chelator, was also supplemented into the medium to further remove the extracellular Ca^{2+} trapped in the cartilage by the negative charges on glycosaminoglycan (GAG) chains. (2) ER calcium store: Cartilage explants were incubated in 1 μM thapsigargin to deplete the calcium stored in the ER, which is the major intracellular calcium store in chondrocytes (29). As the vehicle control for thapsigargin treated samples, cartilage samples were incubated in DMEM supplemented with 0.25% v/v DMSO. (3) PLC-IP_3 pathway: Cartilage sample was incubated in 11 mM neomycin to inhibit the phospholipase C (PLC) from hydrolyzing phospholipids into inositol triphosphate (IP_3) and diacylglycerol (DAG). IP_3 can induce the calcium release from ER. (4) P2 purinoceptors: PPADS (pyridoxalphosphate-6-azophenyl-2′,4′-disulfonic acid) was employed to inhibit the P2 receptors on the cell membrane (167 μM) (19). Although PPADS is known as a P2X inhibitor, it does not completely discriminate between P2X and P2Y receptors. Here, PPADS is utilized as a non-selective antagonist for all P2 receptors (30). (5) Mechanosensitive ion channels: Gadolinium chloride ($GdCl_3$, 10 μM) was applied to the cartilage explants to inhibit the mechanosensitive ion channels on the plasma membrane (22). (6) T-type voltage gated calcium channel (VGCC): NNC55-0396 (17.7 μM) was supplied in the medium to block the T-type VGCCs on chondrocytes (28). (7) TRPV4 channel: GSK205 (10 μM) was introduced to cartilage explants to deactivate the TPRV4 channel (10). According to the calcium imaging setup and molecular weights of seven chemicals, it was estimated that all chemicals can reach the imaged chondrocytes in a few seconds. During the calcium imaging of the treated and control samples, compressive loading was applied to the sample following the loading profile described above.

2.4. Data Analysis and Statistics

For each cartilage explant, 50–100 cells located in the center of the imaging area along the thickness direction were analyzed. The total number of explants and cells analyzed for the seven $[Ca^{2+}]_i$ signaling pathways was listed in Table 1. For each cell, $[Ca^{2+}]_i$ concentration oscillation was represented by the fluorescent signal intensity of its transients. A cell was defined as responsive if a calcium peak was released with a magnitude four times higher than the maximum fluctuation along the baseline (15). The fraction of responsive cells over total cells was calculated as the responsive rate of a sample. For all responsive cells, the number of $[Ca^{2+}]_i$ peaks during the 16 min loading period was counted. Three extra temporal features of the $[Ca^{2+}]_i$ peaks, including the time to reach a peak (t_1), relaxation time from a peak (t_2), and time interval between two neighboring peaks (t_3), were extracted and compared between the control and treated samples as described in our previous studies (11; 27) (Fig. 2B). Pearson's chi-squared test was utilized to detect the significant difference in the responsive rate between groups. To characterize the intrinsic variation among individual explant, a linear mixed effects model was used to compare the temporal parameters of $[Ca^{2+}]_i$ signaling. The effects of antagonist treatment on cartilage explant was set as a fixed, constant factor; while the individual explant was set as a random factor by assuming a different baseline of $[Ca^{2+}]_i$ parameters for each individual cartilage explant. All data were shown as mean ± SEM. Statistical significance was indicated when P<0.05.

3. RESULTS

3.1. Mechanical Loading Enhanced $[Ca^{2+}]_i$ Signaling

The time-lapse images of a sample are shown in Fig. 2A. Four cells showing $[Ca^{2+}]_i$ oscillations were marked by white arrows (Fig. 2A). $[Ca^{2+}]_i$ oscillation of a cell can be obtained by measuring the average image intensity of each cell in all time-lapse images (Fig. 2B). Typical transient curves of $[Ca^{2+}]_i$ intensity in chondrocytes, loaded or unloaded, were presented in Fig. 3A. Cells under both conditions demonstrated prominent $[Ca^{2+}]_i$ oscillations with repetitive and spike-like $[Ca^{2+}]_i$ peaks. The responsive rate of loaded cells was 23.7±1.4%, significantly higher than the spontaneous responsive rate of the non-loaded cells (16.8±1.2%, P=0.008). The average numbers of multiple $[Ca^{2+}]_i$ peaks per responsive cell were similar between two groups, 2.5±0.17 for the loaded group and 2.5±0.18 for the unloaded group (P>0.05). Consistently, there was no significant difference in the time interval of two neighboring peaks (t_3) between the two groups (P>0.05, Fig. 3B). It took the loaded chondrocytes significantly shorter time to relax from $[Ca^{2+}]_i$ peaks than the cells in control group (t_2: 14.6±0.9 s vs. 19.9 ±1.6 s, P=0.005).

3.2. Extracellular Calcium Influx

Treatment of EGTA that chelated the extracellular Ca^{2+} in medium almost abolished the $[Ca^{2+}]_i$ signaling of *in situ* chondrocytes under compressive loading. Only 2 out of 216 cells exhibited $[Ca^{2+}]_i$ oscillation with a single peak, which was significantly lower than that of the control group (29.5±2.1% for responsive rate, P<0.001; 3.0±0.25 for number of peaks, P=0.007) (Fig. 4). The limited number of responsive cells (n = 2) in the EGTA treated group hindered further comparison of the temporal parameters between two groups.

3.3. Roles of ER Calcium Store

Depletion of the ER store by thapsigargin significantly reduced the $[Ca^{2+}]_i$ responsive rate of *in situ* chondrocytes under loading ($5.2\pm0.75\%$ vs. $23.5\pm1.4\%$ in the control, P<0.001; Fig. 5A). DMSO-treated samples showed similar calcium responsive rate as the non-DMSO treated samples, which were randomly selected from the other groups without DMSO supplement ($23.5\pm1.42\%$ vs $23.7\pm1.43\%$, n = 5; P>0.05). A consistent phenomenon was observed when the PLC-IP$_3$ pathway was blocked by neomycin ($7\pm0.84\%$ vs. $34.3\pm1.6\%$ in the control, P<0.001) (Fig. 5B). The responsive cells treated by neomycin also presented a lower number of peaks compared to the control (1.8 ± 0.26 vs. 2.9 ± 0.22; P=0.001) and an increased time interval between peaks (152.70 ± 2.26 vs. 211.02 ± 4.22; P=0.03). Compared to the thapsigargin and neomycin treatments, PPADS exerted weaker inhibitory effects on the intracellular Ca^{2+} release. $24.2\pm2.2\%$ of cells presented $[Ca^{2+}]_i$ responses in the PPADS treated group compared to $38.8\pm2.5\%$ responsive cells in the untreated control (P=0.003, Fig. 4C). Under compressive loading, none of the three drugs exerted substantial effects on the $[Ca^{2+}]_i$ temporal parameters compared to those of the untreated control samples.

3.4. Ion Channels on Plasma Membrane

Blocking the mechanosensitive ion channels by GdCl$_3$ significantly reduced the responsive rate in loaded chondrocytes ($17.0\pm1.5\%$ vs. $28.9\pm1.8\%$ in the untreated group, P<0.001, Fig. 6A), but didn't affect the number of $[Ca^{2+}]_i$ peaks or other temporal parameters (P>0.05). Treatment with NNC-55-0936, a selective blocker of T-type VGCCs, also inhibited the *in situ* chondrocytes from releasing $[Ca^{2+}]_i$ peaks under compression ($14.4\pm1.5\%$ vs. $30.2\pm1.9\%$ for responsive rate, P<0.001, Fig. 6B). The blockage of TRPV4 channels by GSK205 prominently reduced the proportion of chondrocytes with $[Ca^{2+}]_i$ responses under compressive loading, as only $6\%\pm0.76\%$ of cells responded ($18.3\pm1.9\%$ in control, P<0.001) (Fig. 6C). Interestingly, the relaxation duration of $[Ca^{2+}]_i$ peaks was significantly shortened when the TRPV4 channel was blocked (P=0.03). These results indicated the important role of TRPV4 channel in regulating the temporal rhythm of $[Ca^{2+}]_i$ signaling.

4. Discussion

Metabolic activities of chondrocytes are extensively regulated by the mechanical and other physical stimuli from the ECM and surrounding fluid. The profiles and magnitudes of these stimuli are dependent on the unique composition, nanostructure, organization, and mechanical behaviors of the peri- and extra-cellular matrix. In addition, phenotype and mechanobiology behaviors of chondrocytes change with the surrounding environment. Therefore, primary chondrocytes cultured in monolayer, 3-dimentional hydrogel, and residing in their native environment could have distinct responses to identical physical stimuli. As a soft connective tissue, cartilage deforms easily over 10% strain in its daily activities, which makes the microscopy recording of the cell activities in its natural environment challenging. In this study, a bi-directional loading device was built to minimize the movement of tissue in the center of loaded cartilage sample, so that the calcium imaging of *in situ* chondrocytes can be recorded. Compressive loading was chosen here as it is the dominant physiological loading pattern on articular cartilage.

Under compression, a number of physical stimuli are generated and applied on the chondrocytes. Although mechanical loading on cell body can induce vigorous $[Ca^{2+}]_i$ responses, actual stress or strain on the cell body could be much lower than those of the ECM due to the presence of a pericellular matrix, which functions as a soft cushion surrounding the chondrocyte and dampens the actual loading on the cell body in a largely deformed cartilage (31; 32). Deformation of *in situ* chondrocytes was found to be lower than the ECM strain in an experimental study (33). A 15% compressive strain in ECM may resulted in merely 9% compression of cell height. Therefore, the actual decrease of chondrocyte height could be lower than 10% in the present study. In contrast to the dampened stress and strain on chondrocytes, ascent of hydrostatic pressure in the loaded cartilage can be fully sensed by the cells and induce $[Ca^{2+}]_i$ responses. Compression of ECM can squeeze the interstitial fluid out of the cartilage, which in theory should generate fluid flow or shear stress on cell membrane. Due to the low permeability of ECM, fluid flow speed in the loaded cartilage is extremely slow and at tens of nanometers per second (34; 35), and the resulting fluid shear stress on cell membrane is negligible in comparison to those studies of fluid flow induced calcium signaling (~5-40 dynes/cm^2). Thus fluid flow might be a minor stimulation responsible for the $[Ca^{2+}]_i$ responses of *in situ* chondrocytes.

The extracellular matrix of cartilage is negatively charged due to the presence of GAG chains. The fixed charges in ECM attract extra cations into the tissue and further generate the so-called Donnan's osmotic pressure in cartilage (2). Compression of the ECM increases the density of fixed charges (~12% increase at 10% volume change of ECM), which causes a cascade of mechano-electrochemical stimuli on the chondrocytes. First, higher fixed charge density will result in higher osmotic pressure, which represents a major source of osmotic stress on chondrocytes. Osmotic stress can induce vigorous $[Ca^{2+}]_i$ responses in chondrocytes due to the presence of TRPV4 channels (10). As the PCM of chondrocytes is much softer than the ECM, volume of chondrocytes can easily expand or shrink under different osmolarity, which can further activate the mechanosensitive channels on plasma membrane. Second, denser fixed charges will attract more cations to maintain electric neutrality. Fluctuation of cation concentration can activate calcium or ion channels on the plasma membrane and cause Ca^{2+} influx (22). Third, increased fixed charge density changes the electrical potential across the ECM at millivolt level (36), which represents another strong stimulation for $[Ca^{2+}]_i$ responses (12). Lastly, due to the unbalanced free cations and anions in the fluid phase, compression of ECM results in both streaming potential and diffusion potential across the tissue (37). All of these mechano-electrochemical stimuli, especially the stress/strain (8; 38), osmotic stress (9; 10), and electric potential (12), could be responsible for the promoted $[Ca^{2+}]_i$ signaling in the loaded cartilage as observed in this study.

Temporal features of the $[Ca^{2+}]_i$ peaks in the loaded cartilage are different to those in the unloaded tissue. The relaxation time, defined as the time for a $[Ca^{2+}]_i$ peak relaxing from the highest value to its 50%, is significantly shortened in the loaded sample. This finding is consistent with a previous study using chondrocyte-agarose model subjected to cyclic compression (4). Mechanical loading induced stimuli, as aforementioned, could activate or open extra ion channels on the plasma membrane, which accelerate the influx and efflux of Ca^{2+}. Moreover, as mechanical loading promotes the convection and diffusion of free Ca^{2+}

in ECM, abundant extracellular Ca^{2+} may also attribute to the short duration of $[Ca^{2+}]_i$ peaks. In this study, mechanical loading had no significant effect on the frequency of $[Ca^{2+}]_i$ peaks or the time interval between two neighboring peaks. Therefore, the refractory time after a $[Ca^{2+}]_i$ peak is not changed in chondrocytes by the mechanical loading, which was also observed in literature (4).

Although the increase of $[Ca^{2+}]_i$ has two sources, the extracellular Ca^{2+} influx and the release of intracellular store, removal of extracellular Ca^{2+} with EGTA almost completely abolished the $[Ca^{2+}]_i$ signaling of *in situ* chondrocytes. According to the results in this study, $[Ca^{2+}]_i$ signaling of chondrocytes, either spontaneous or load induced, has to be initiated by the extracellular Ca^{2+} influx. Previous studies also found that deformation of chondrocyte surface cannot induce any $[Ca^{2+}]_i$ responses after removing the extracellular Ca^{2+}, even with the presence of full intracellular calcium stores (4; 22). We also noticed that osteocytes and osteoblasts have no $[Ca^{2+}]_i$ responses under fluid flow or AFM indenting in Ca^{2+} free medium (27; 39). In this study, when cartilage was balanced in abundant Ca^{2+} free medium, $[Ca^{2+}]_i$ responses can still be observed in the chondrocytes unless extra EGTA was supplemented into the medium (results not shown). Due to the negatively charged nature of ECM, Ca^{2+} can be tightly trapped inside cartilage. It is difficult to fully deplete the interstitial Ca^{2+} by putting the tissue in Ca^{2+} free medium. In contrast, EGTA can actively chelate and deplete the trapped Ca^{2+}. $[Ca^{2+}]_i$ signaling of *in situ* chondrocytes observed in the Ca^{2+} free medium also implies that even a low density of extracellular Ca^{2+} is sufficient to initiate the $[Ca^{2+}]_i$ responses in chondrocytes. This may explain the significantly reduced, but not completely abolished, $[Ca^{2+}]_i$ responses found in the Ca^{2+} depleted environment using chondrocyte-agarose construct models (4; 38).

Significant inhibitory effects on $[Ca^{2+}]_i$ responses were observed by blocking purinergic receptors, depletion of ER store, or inhibition of PLC-IP$_3$ pathway of *in situ* chondrocytes, which are consistent with previous studies (4; 29). Influx of Ca^{2+} can stimulate vesicular ATP release, which in turn activates the purinergic (P2) receptors on cell membrane (19). P2X, one of the five subclasses of P2 family, are ligand-gated nonselective ion channels, which can directly facilitate extracellular Ca^{2+} influx. In contrast, activation of P2Y receptors results in the Ca^{2+} release from ER via PLC-IP$_3$ pathway. Therefore, extracellular ATP has the capability to induce full $[Ca^{2+}]_i$ responses in cells (4). Moreover, as a small molecule, ATP can easily diffuse or transport in fluid to neighboring cells. We have reported that extracellular ATP diffusion is a major mechanism facilitating the calcium wave propagation across the cell networks (39; 40). In this study, responsive rate of chondrocytes was significantly reduced when ATP-related pathway was interrupted. Therefore, the calcium signaling observed in the loaded cartilage are not all induced by the mechanical loading or related stimuli. $[Ca^{2+}]_i$ responses of many chondrocytes are actually initiated by the release of ATP from neighboring cells, while the mechanical loading could promote the diffusion and convection of ATP in the ECM. This study demonstrated that extracellular ATP serves as an essential second messenger for cell-cell communication among the isolated chondrocytes.

TRPV4 ion channel can be activated by various stimuli, including osmotic stress, mechanical loading, and heat. TRPV4 plays a key role in regulating calcium homeostasis

and matrix metabolism in cartilage (10; 41), while TRPV4-dysfunction is associated with the development of osteoarthritis (42–44). In the compressed cartilage, both mechanical loading and osmotic stress can activate the TRPV4 channel and initiate the $[Ca^{2+}]_i$ transients. In this study, inhibition of TRPV4 significantly reduced the $[Ca^{2+}]_i$ responses in loaded cartilage. In addition, TRPV4 is believed to be a slow non-selective ion channel, as a delay in response to osmotic stimulation was observed in TRPV4-expressing cells (45). This feature may attribute to the shortened rising time of $[Ca^{2+}]_i$ peak in the TRPV4-blocked chondrocytes. Mechanosensitive ion channels on the cell membrane are believed to be responsible for the mechanotransduction of most musculoskeletal cells. The treatment of cartilage explants with gadolinium led to a significantly decreased percentage of cells responding to the compressive loading. This is consistent with most of the previous studies (4; 38). Recently, PIEZO1 and PIEZO2 are identified as two mechanosensitive channels on chondrocytes, which have to work synergistically to initiate the $[Ca^{2+}]_i$ responses in the loaded cells (17). Future study is of necessity to understand the roles of different mechanosensitive channels in the $[Ca^{2+}]_i$ signaling of *in situ* chondrocytes (22). Another important finding is that T-type VGCCs play a critical role in chondrocyte $[Ca^{2+}]_i$ signaling. T-type VGCC is activated by low voltage stimulation followed by depolarization of the plasma membrane and elevation of $[Ca^{2+}]_i$ concentration (46). The physiological roles of T-type channels are often accomplished by the distinctive low activation threshold of these channels, which boosts up membrane depolarization in excitable cells. In this study, inhibition of T-type VGCC on chondrocytes reduced the $[Ca^{2+}]_i$ responsive percentage by ~50%, implying that a large number of chondrocytes are relying on the activation of T-type VGCCs to initiate the $[Ca^{2+}]_i$ responses under loading, although chondrocyte is often regarded as non-excitable cells. Our recent study also found that inhibition of T-type VGCCs suppressed the OA progression in meniscus dislocated mouse model (18).

There are several limitations we would like to point out regarding this study. First, to study the mature chondrocytes in the middle layer of cartilage, a cross section area had to be created for imaging the cells underneath the cutting surface. This sample preparation process may affect the mechanical behaviors of cartilage and chondrocyte cellular responses to mechanical stimuli when the tissue was loaded. Calcium signaling of superficial zone chondrocytes has been studied *in situ* previously (5). The middle zone cartilage, with randomly oriented collagen fibrils, serves as the first line of resistance to compressive forces. Therefore, it is also important to understand the mechanobiology behaviors of mature chondrocytes in the middle layer. Second, although the 10% compressive strain on cartilage was physiologically relevant, the loading rate in this study was non-dynamic, much slower compared to that during daily activities. This loading protocol was designed to assist the imaging of the same cell population during the entire loading phase. In the middle of imaging area, the displacement of chondrocytes was minimized by the slow, bi-directional loading profile; whereas the residual displacement at a fast speed could still affect the track and imaging of chondrocytes.

In conclusion, a new microscopy loading device was built to record the $[Ca^{2+}]_i$ responses of *in situ* chondrocytes in the loaded cartilage. Compressive loading induced $[Ca^{2+}]_i$ responses in more chondrocytes and also shortened the duration of $[Ca^{2+}]_i$ peaks in comparison to the non-loaded tissues. Roles of seven pathways in chondrocyte $[Ca^{2+}]_i$ signaling were

identified. Extracellular Ca^{2+} influx is required for the initiation of $[Ca^{2+}]_i$ transients. Diffusion of extracellular ATP represents an essential mechanism for the intercellular communication between chondrocytes. TRPV4, mechanosensitive, and T-type VGCC ion channels on plasma membrane all play critical roles in the initiation of $[Ca^{2+}]_i$ signaling in the chondrocytes.

Acknowledgments

References

1. Guilak F, Butler DL, Goldstein SA, Baaijens FP. Biomechanics and mechanobiology in functional tissue engineering. J Biomech. 2014; 47:1933–1940. [PubMed: 24818797]

2. Mow, VC., Gu, W., Chen, F. Structure and function of articular cartilage and meniscus. In: Mow, VC., Huiskes, R., editors. Basic orthopaedic biomechanics & mechano-biology. Third. 2005. p. 1online resource (736 pages)

3. Chen X, Zhou Y, Wang L, et al. Determining Tension-Compression Nonlinear Mechanical Properties of Articular Cartilage from Indentation Testing. Annals of biomedical engineering. 2016; 44:1148–1158. [PubMed: 26240062]

4. Pingguan-Murphy B, El-Azzeh M, Bader DL, Knight MM. Cyclic compression of chondrocytes modulates a purinergic calcium signalling pathway in a strain rate- and frequency-dependent manner. J Cell Physiol. 2006; 209:389–397. [PubMed: 16883605]

5. Madden RM, Han SK, Herzog W. The effect of compressive loading magnitude on in situ chondrocyte calcium signaling. Biomechanics and modeling in mechanobiology. 2015; 14:135–142. [PubMed: 24853775]

6. Han SK, Wouters W, Clark A, Herzog W. Mechanically induced calcium signaling in chondrocytes in situ. Journal of orthopaedic research : official publication of the Orthopaedic Research Society. 2012; 30:475–481. [PubMed: 21882238]

7. Edlich M, Yellowley CE, Jacobs CR, Donahue HJ. Oscillating fluid flow regulates cytosolic calcium concentration in bovine articular chondrocytes. J Biomech. 2001; 34:59–65. [PubMed: 11425081]

8. Browning JA, Saunders K, Urban JP, Wilkins RJ. The influence and interactions of hydrostatic and osmotic pressures on the intracellular milieu of chondrocytes. Biorheology. 2004; 41:299–308. [PubMed: 15299262]

9. Chao PH, West AC, Hung CT. Chondrocyte intracellular calcium, cytoskeletal organization, and gene expression responses to dynamic osmotic loading. Am J Physiol Cell Physiol. 2006; 291:C718–725. [PubMed: 16928775]

10. O'Conor CJ, Leddy HA, Benefield HC, et al. TRPV4-mediated mechanotransduction regulates the metabolic response of chondrocytes to dynamic loading. Proceedings of the National Academy of Sciences of the United States of America. 2014; 111:1316–1321. [PubMed: 24474754]

11. Zhou Y, David MA, Chen X, et al. Effects of Osmolarity on the Spontaneous Calcium Signaling of In Situ Juvenile and Adult Articular Chondrocytes. Annals of biomedical engineering. 2016; 44:1138–1147. [PubMed: 26219403]

12. Xu J, Wang W, Clark CC, Brighton CT. Signal transduction in electrically stimulated articular chondrocytes involves translocation of extracellular calcium through voltage-gated channels. Osteoarthritis and cartilage. 2009; 17:397–405. [PubMed: 18993082]

13. Varady NH, Grodzinsky AJ. Osteoarthritis year in review 2015: mechanics. Osteoarthritis and cartilage. 2016; 24:27–35. [PubMed: 26707990]

14. Kono T, Nishikori T, Kataoka H, et al. Spontaneous oscillation and mechanically induced calcium waves in chondrocytes. Cell Biochem Funct. 2006; 24:103–111. [PubMed: 16342135]

15. Zhou Y, Park M, Cheung E, et al. The effect of chemically defined medium on spontaneous calcium signaling of in situ chondrocytes during long-term culture. J Biomech. 2015; 48:990–996. [PubMed: 25700610]

16. Clapham DE. Calcium signaling. Cell. 2007; 131:1047–1058. [PubMed: 18083096]

17. Lee W, Leddy HA, Chen Y, et al. Synergy between Piezo1 and Piezo2 channels confers high-strain mechanosensitivity to articular cartilage. Proceedings of the National Academy of Sciences of the United States of America. 2014; 111:E5114–5122. [PubMed: 25385580]

18. Srinivasan PP, Parajuli A, Price C, et al. Inhibition of T-Type Voltage Sensitive Calcium Channel Reduces Load-Induced OA in Mice and Suppresses the Catabolic Effect of Bone Mechanical Stress on Chondrocytes. PloS one. 2015; 10:e0127290. [PubMed: 26011709]

19. Millward-Sadler SJ, Wright MO, Flatman PW, Salter DM. ATP in the mechanotransduction pathway of normal human chondrocytes. Biorheology. 2004; 41:567–575. [PubMed: 15299287]

20. Vandenburgh HH, Shansky J, Karlisch P, Solerssi RL. Mechanical stimulation of skeletal muscle generates lipid-related second messengers by phospholipase activation. J Cell Physiol. 1993; 155:63–71. [PubMed: 8468370]

21. Qusous A, Parker E, Ali N, et al. The effects of REV5901 on intracellular calcium signalling in freshly isolated bovine articular chondrocytes. Gen Physiol Biophys. 2012; 31:299–307. [PubMed: 23047943]

22. Guilak F, Zell RA, Erickson GR, et al. Mechanically induced calcium waves in articular chondrocytes are inhibited by gadolinium and amiloride. Journal of orthopaedic research : official publication of the Orthopaedic Research Society. 1999; 17:421–429. [PubMed: 10376733]

23. Kerrigan MJ, Hall AC. Control of chondrocyte regulatory volume decrease (RVD) by $[Ca^{2+}]_i$ and cell shape. Osteoarthritis and cartilage. 2008; 16:312–322. [PubMed: 17855127]

24. Kerrigan MJ, Hook CS, Qusous A, Hall AC. Regulatory volume increase (RVI) by in situ and isolated bovine articular chondrocytes. J Cell Physiol. 2006; 209:481–492. [PubMed: 16897756]

25. Gao Y, Liu S, Huang J, et al. The ECM-cell interaction of cartilage extracellular matrix on chondrocytes. Biomed Res Int. 2014; 2014:648459. [PubMed: 24959581]

26. Bian L, Stoker AM, Marberry KM, et al. Effects of dexamethasone on the functional properties of cartilage explants during long-term culture. Am J Sports Med. 2010; 38:78–85. [PubMed: 19959744]

27. Lu XL, Huo B, Park M, Guo XE. Calcium response in osteocytic networks under steady and oscillatory fluid flow. Bone. 2012; 51:466–473. [PubMed: 22750013]

28. Lu XL, Huo B, Chiang V, Guo XE. Osteocytic network is more responsive in calcium signaling than osteoblastic network under fluid flow. Journal of bone and mineral research : the official journal of the American Society for Bone and Mineral Research. 2012; 27:563–574.

29. Hung CT, Allen FD, Mansfield KD, Shapiro IM. Extracellular ATP modulates $[Ca^{2+}]_i$ in retinoic acid-treated embryonic chondrocytes. Am J Physiol. 1997; 272:C1611–1617. [PubMed: 9176153]

30. Lambrecht G, Friebe T, Grimm U, et al. PPADS, a novel functionally selective antagonist of P2 purinoceptor-mediated responses. Eur J Pharmacol. 1992; 217:217–219. [PubMed: 1330591]

31. Wilusz RE, Zauscher S, Guilak F. Micromechanical mapping of early osteoarthritic changes in the pericellular matrix of human articular cartilage. Osteoarthritis and cartilage. 2013; 21:1895–1903. [PubMed: 24025318]

32. Korhonen RK, Herzog W. Depth-dependent analysis of the role of collagen fibrils, fixed charges and fluid in the pericellular matrix of articular cartilage on chondrocyte mechanics. J Biomech. 2008; 41:480–485. [PubMed: 17936762]

33. Madden R, Han SK, Herzog W. Chondrocyte deformation under extreme tissue strain in two regions of the rabbit knee joint. J Biomech. 2013; 46:554–560. [PubMed: 23089458]

34. Zimmerman BK, Bonnevie ED, Park M, et al. Role of interstitial fluid pressurization in TMJ lubrication. Journal of dental research. 2015; 94:85–92. [PubMed: 25297115]

35. Ateshian GA, Costa KD, Hung CT. A theoretical analysis of water transport through chondrocytes. Biomechanics and modeling in mechanobiology. 2007; 6:91–101. [PubMed: 16705444]

36. Garon M, Legare A, Guardo R, et al. Streaming potentials maps are spatially resolved indicators of amplitude, frequency and ionic strength dependant responses of articular cartilage to load. J Biomech. 2002; 35:207–216. [PubMed: 11784539]

37. Lai WM, Mow VC, Sun DD, Ateshian GA. On the electric potentials inside a charged soft hydrated biological tissue: streaming potential versus diffusion potential. J Biomech Eng. 2000; 122:336–346. [PubMed: 11036556]

38. Roberts SR, Knight MM, Lee DA, Bader DL. Mechanical compression influences intracellular Ca^{2+} signaling in chondrocytes seeded in agarose constructs. J Appl Physiol. 2001; 90:1385–1391. [PubMed: 11247938]

39. Huo B, Lu XL, Costa KD, et al. An ATP-dependent mechanism mediates intercellular calcium signaling in bone cell network under single cell nanoindentation. Cell Calcium. 2010; 47:234–241. [PubMed: 20060586]

40. Huo B, Lu XL, Guo XE. Intercellular calcium wave propagation in linear and circuit-like bone cell networks. Philos T R Soc A. 2010; 368:617–633.

41. Phan MN, Leddy HA, Votta BJ, et al. Functional characterization of TRPV4 as an osmotically sensitive ion channel in porcine articular chondrocytes. Arthritis Rheum. 2009; 60:3028–3037. [PubMed: 19790068]

42. Hurd L, Kirwin SM, Boggs M, et al. A mutation in TRPV4 results in altered chondrocyte calcium signaling in severe metatropic dysplasia. Am J Med Genet A. 2015; 167A:2286–2293. [PubMed: 26249260]

43. Kanju P, Chen Y, Lee W, et al. Small molecule dual-inhibitors of TRPV4 and TRPA1 for attenuation of inflammation and pain. Scientific reports. 2016; 6:26894. [PubMed: 27247148]

44. Rocio Servin-Vences M, Moroni M, Lewin GR, Poole K. Direct measurement of TRPV4 and PIEZO1 activity reveals multiple mechanotransduction pathways in chondrocytes. Elife. 2017; 6

45. Plant, TD., Strotmann, R. TRPV4: A Multifunctional Nonselective Cation Channel with Complex Regulation. In: Liedtke, WB., Heller, S., editors. TRP Ion Channel Function in Sensory Transduction and Cellular Signaling Cascades. Boca Raton (FL): 2007.

46. Nilius B, Talavera K, Verkhratsky A. T-type calcium channels: The never ending story. Cell Calcium. 2006; 40:81–88. [PubMed: 16797069]
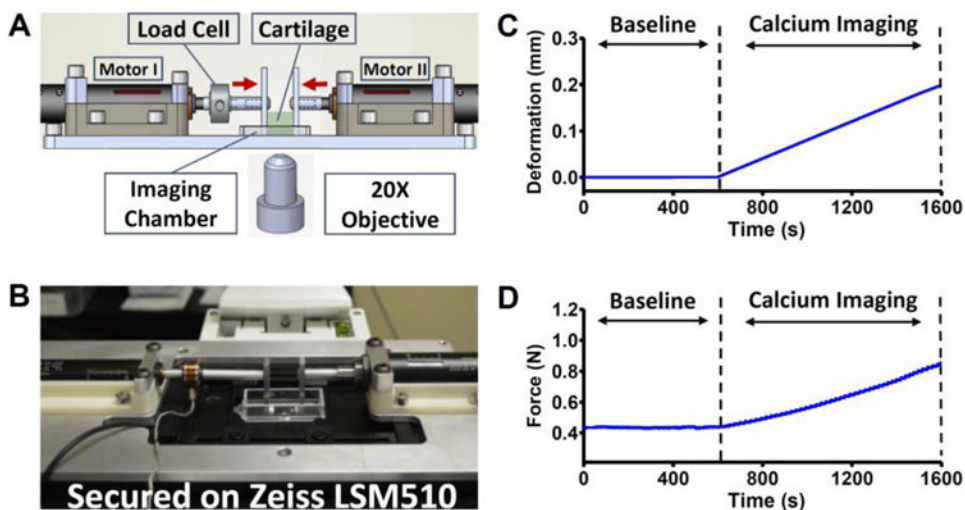
Figure 1.
A bidirectional microscopy loading device for cartilage explant. (A) A schematic illustration of the device. Cartilage sample is placed in an imaging chamber and submerged in medium. Two parallel loading platens on both sides of the sample are driven by two coaxial motors, respectively. Load cell can record the responding force from cartilage. All components are fixed on a based plate, which itself can be mounted on the X-Y stage of a microscope. (B) A picture of the loading device mounted on a confocal microscope (Zeiss LSM510). (C) Loading profile during the calcium imaging of the cartilage sample. Tissue was compressed at 0.2 μm/s for 1,000 seconds (~10% compression of the cartilage explant). (D) A typical force response curve of the cartilage sample under the compressive loading. Due to the slow loading rate, increase of responding force is close to a linear curve.
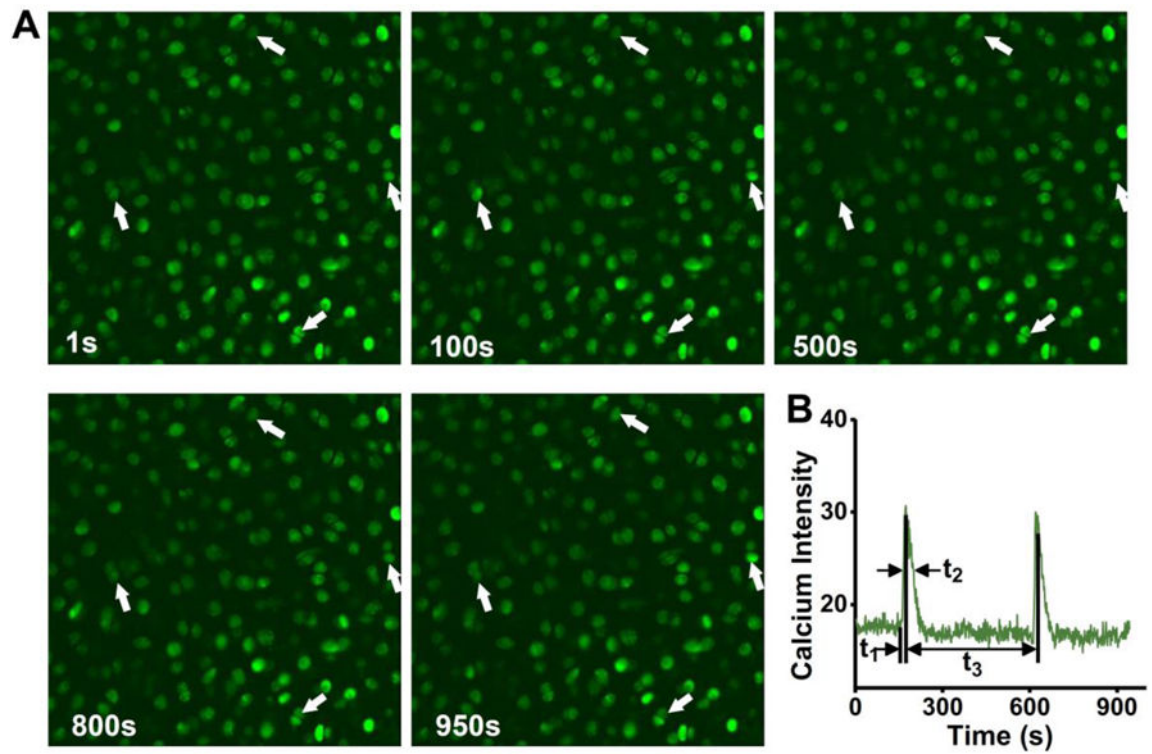
Figure 2.
$[Ca^{2+}]_i$ responses of *in situ* chondrocytes in a loaded cartilage explant. (A) Calcium images of the chondrocytes stained with Fluo 8 AM at five different time points taken by confocal microscope. White arrows highlight cells with oscillating $[Ca^{2+}]_i$ concentration. Some cells showed multiple calcium peaks. Scales bars = 50 μm. (B) A typical $[Ca^{2+}]_i$ transient of chondrocyte in cartilage. The characteristic temporal parameters are defined. t_1 denotes the time from baseline to the maximum value of the peak. t_2 is the time from peak value to the 50% relaxation. t_3 is the time interval between two neighboring peaks.
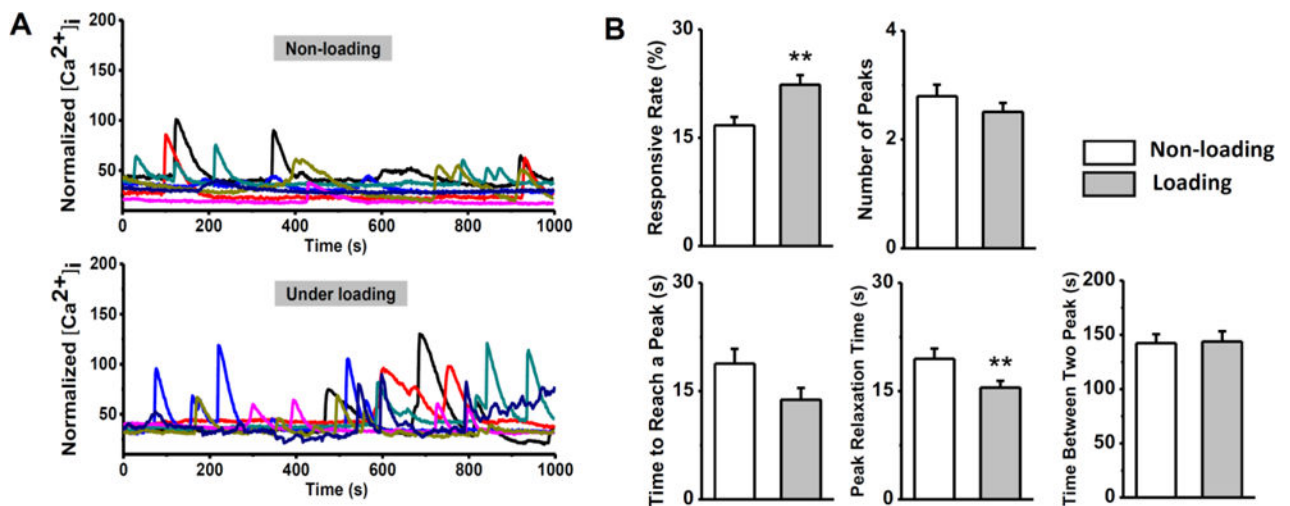
Figure 3.
Comparison of $[Ca^{2+}]_i$ signaling of *in situ* chondrocytes in the loaded and unloaded cartilage explants. (A) Typical $[Ca^{2+}]_i$ intensity curves of chondrocytes in 1,000 seconds from the loaded and unloaded groups. Each curve represents the calcium transient of a single cell. A large number of chondrocytes can release multiple $[Ca^{2+}]_i$ peaks in 1,000 seconds. (B) Percentage of chondrocytes showed $[Ca^{2+}]_i$ peaks in loaded cartilage is significantly higher than the unloaded sample, while the average number of peaks in each responsive cell had no difference. Temporal parameters of $[Ca^{2+}]_i$ peaks, including time to reach a peak, peak relaxation time, and time between two peaks are compared between two groups. *: P value < 0.05; **: P value < 0.01; and ***: P value < 0.001.
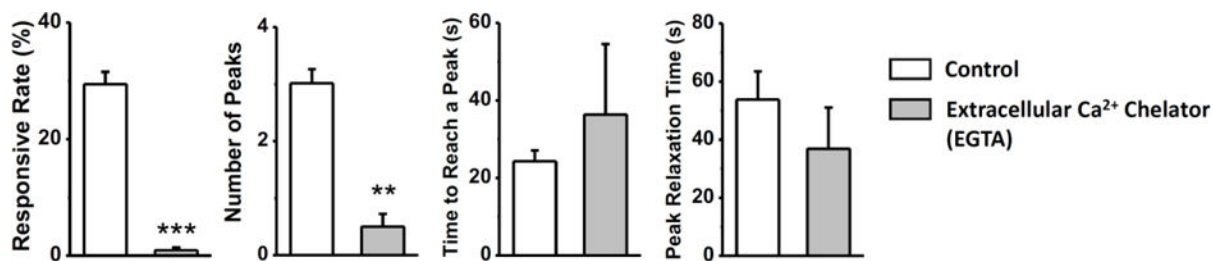
Figure 4.
Role of extracellular Ca^{2+} source in the $[Ca^{2+}]_i$ responses of *in situ* chondrocytes in loaded cartilage explants. Few chondrocytes can have $[Ca^{2+}]_i$ transients after the depletion of extracellular Ca^{2+} in the medium. No responsive cells can have multiple $[Ca^{2+}]_i$ peaks (time between peaks not showing). Time to reach a peak and peak relaxation time of responsive cells have no difference between the two groups. *: P value < 0.05; **: P value < 0.01; and ***: P value < 0.001.
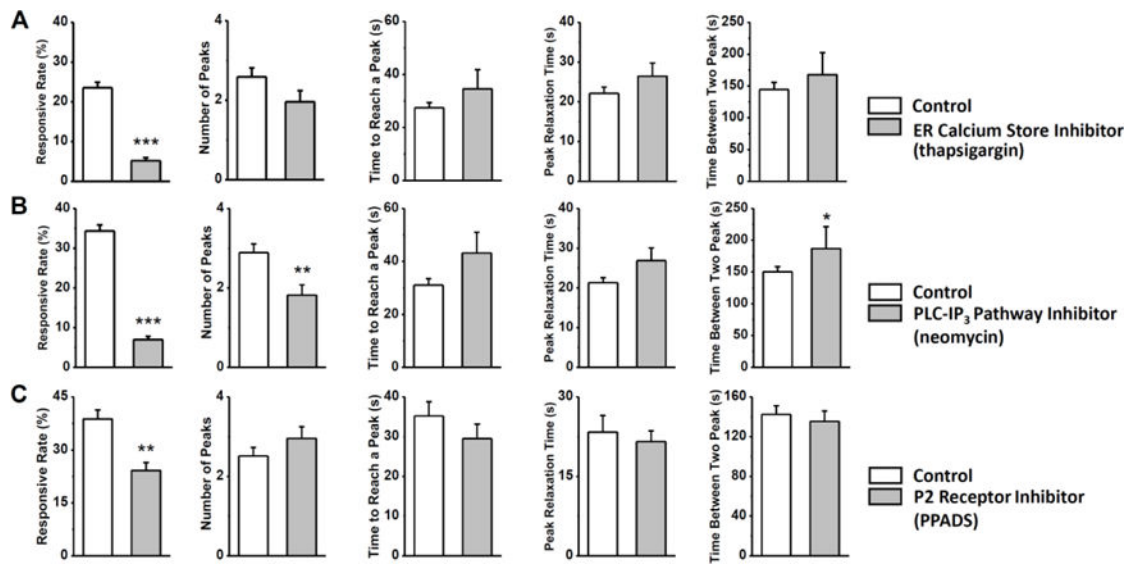
Figure 5.
Role of P2 receptors and intracellular ER calcium release in the $[Ca^{2+}]_i$ responses of *in situ* chondrocytes. Cartilage explants are loaded in both control and chemical treated groups. (A) $[Ca^{2+}]_i$ responses after the ER calcium store was depleted by thapsigargin. (B) $[Ca^{2+}]_i$ responses with inhibited PLC-IP$_3$ activities by neomycin. (C) $[Ca^{2+}]_i$ responses with the presence of PPADS, a P2 receptor inhibitor. *: P value < 0.05; **: P value < 0.01; and ***: P value < 0.001.
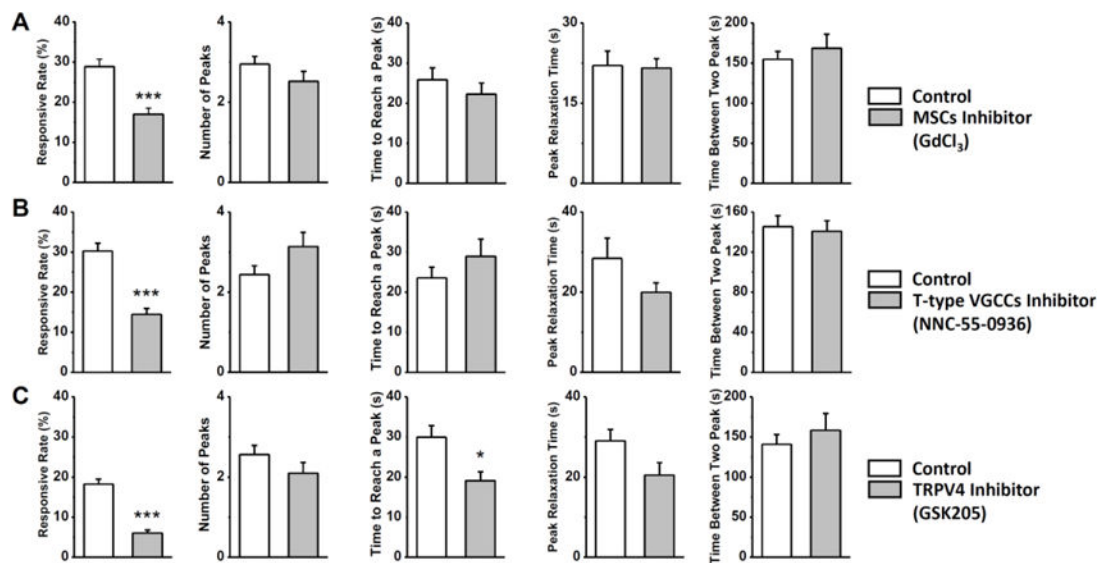
Figure 6.
Role of three nonselective ion channels in the $[Ca^{2+}]_i$ responses of *in situ* chondrocytes. Cartilage explants are loaded in both control and chemical treated groups. (A) $[Ca^{2+}]_i$ responses with the mechanosensitive channels blocked by gadolinium. (B) $[Ca^{2+}]_i$ responses with the T-type VGCCs blocked by NNC55-0396. (C) $[Ca^{2+}]_i$ responses with the TRPV4 channel blocked by GSK205. *: P value < 0.05; **: P value < 0.01; and ***: P value < 0.001.

Table 1

Number of the total cartilage explants and chondrocytes analyzed in $[Ca^{2+}]_i$ signaling for seven pathways.

	Extracellular Ca^{2+}	ER store	PLC-IP$_3$	P2 receptor	Mechanosensitive ion channel	T-Type VGCC	TRPV4
Explant #	3	5	6	3	5	5	5
Cell # of control group	256	408	495	183	294	281	438
Cell # of drug-treated group	216	480	430	186	335	284	546